J. Condensed Matter Nucl. Sci. 15 (2015) 162–182

Research Article

Hydrogen Embrittlement and Piezonuclear Reactions in Electrolysis Experiments

A. Carpinteri*, O. Borla, A. Manuello and D. Veneziano

Politecnico di Torino, Department of Structural, Geotechnical and Building Engineering, Corso Duca degli Abruzzi, 24–10129 Torino, Italy

A. Goi

Abstract

A great deal of evidence of anomalous nuclear reactions occurring in condensed matter has been observed using electrolysis, fracture (with solids), and cavitation (with liquids). Despite the large amount of experimental results from so-called cold nuclear fusion and Low Energy Nuclear Reaction research activities, researchers still do not understand these phenomena. On the other hand, as reported by most of the articles devoted to Cold Nuclear Fusion, one of the principal features is the appearance of micro-cracks on the electrode surfaces after the experiments. In the present paper, a mechanical explanation is proposed considering a new kind of nuclear reactions, the piezonuclear fission, which is a consequence of hydrogen embrittlement of the electrodes during electrolysis. The experimental activity was conducted using a Ni–Fe anode and a Co–Cr cathode immersed in a potassium carbonate solution. Emissions of neutrons and alpha particles were measured during the experiments and the electrode compositions were analyzed both before and after the electrolysis, revealing the effects of piezonuclear fissions occurring in the host lattices. The symmetrical fission of Ni appears to be the main and most evident feature. Such a reaction would produce two Si atoms or two Mg atoms with additional fragments as alpha particles.
 ISSN 2227-3123

Keywords: Cold nuclear fusion, Electrolysis, Hydrogen embrittlement, Piezonuclear fissions

1. Introduction

During the last two decades a great deal of evidence of anomalous nuclear reactions occurring in condensed matter has been observed [1–34]. These tests were characterized by significant neutron and alpha particle emissions as well as by extra heat generation. At the same time, appreciable variations in the chemical composition after embrittlement or during fatigue fracture were detected [35–40].

Most relevant papers on so-called Cold Nuclear Fusion describe broad experimental activities conducted on electrolytic cells powered by direct current and filled with ordinary or heavy water solutions. In particular, in 1989, Fleischmann and Pons proposed the first experiment reproducing Cold Nuclear Fusion by means of electrolysis [6].

*E-mail: alberto.carpinteri@polito.it

 ISSN 2227-3123

They asserted that the palladium electrode reacted with the deuterium coming from the heavy water solution [6]. Later works reported that Pt and Ti electrodes had also been electrolyzed with D_2O to produce extra energy and chemical elements previously absent [26,28,29]. Extra energy has been also produced from electrolysis with Ni cathodes and H_2O-based electrolyte [13]. Furthermore, it was affirmed that a voltage sufficient to induce plasma generates a large variety of anomalous nuclear reactions when Pd, W, or C cathodes are adopted [16, 21–25].

In many of these experiments, the generated heat was calculated to be several times the input energy and the neutron emissions rate, during electrolysis, was measured to be about three times the natural background level [6]. In 1998, Mizuno presented the results of the measurements conducted by means of neutron emission detectors and compositional analysis techniques related to different electrolytic experiments [22]. Relevant heat generation was observed when the cell was supplied with high voltage, with an excess energy of 2.6 times the input one. Remarkable neutron emissions were revealed during these tests, as well as a considerable amount of new elements, i.e. Pb, Fe, Ni, Cr, and C, with the isotopic distribution of Pb deviating greatly from the natural isotopic abundances [22]. These results suggested that nuclear reactions took place during the electrolysis process [22]. Later, in 2002 Kanarev and Mizuno reported the results obtained from the surface compositional analysis of iron electrodes (99.90% of Fe) immersed in KOH and NaOH solutions [34]. After the experiments, EDX spectroscopy revealed the appearance of several chemical elements previously absent. Concentrations of Si, K, Cr, and Cu were found on the surfaces of the operating cathode immersed in KOH. Analogously, concentrations of Al, Cl, and Ca were noticed on the iron electrode surfaces operating in NaOH. These findings are evidence of compositional changes occurring during plasma formation in electrolysis of water [34]. In 2007, Mosier-Boss et al. [31,33] obtained important proofs of anomalous measurements in experiments conducted by electrolytic co-deposition cells. More in detail, anomalous effects observed in the Pd/D system include heat and helium-4 generation, tritium, neutrons, gamma/X-ray emissions, and transmutations [7,12,31,33].

Preparata wrote: "despite the great amount of experimental results observed by a large number of scientists, a unified interpretation and theory of these phenomena has not been accepted and their comprehension still remains unsolved" [6–9,26,27].

Very recently, theoretical interpretations have been proposed by Widom et al. in order to explain neutron emissions as a consequence of nuclear reactions taking place in iron-rich rocks during brittle micro-cracking and fracture [41,42]. A great deal of evidence shows that iron nuclear disintegrations are observed when rocks containing such nuclei are crushed and fractured. The resulting nuclear transmutations are particularly evident in the case of magnetite rocks and iron-rich materials in general. The same authors argued that neutron emissions may be related to piezoelectric effects and that fission of iron may be a consequence of the photodisintegration of the same nuclei [41].

On the other hand, as shown by most articles devoted to Cold Nuclear Fusion, one of the principal features is the appearance of micro-cracks on electrode surfaces after the tests [26,27]. Such evidence might be directly correlated to hydrogen embrittlement of the material composing the metal electrodes (Pd, Ni, Fe, Ti, etc.). This phenomenon, well-known in metallurgy and fracture mechanics, characterizes metals during forming or finishing operations [43]. In the present study, the host metal matrix (e.g. Pd) is subjected to mechanical damaging and fracturing due to external atoms (deuterium or hydrogen) penetrating into the lattice structure and forcing it apart during gas loading. Hydrogen effects are largely studied especially in metal alloys, where the presence of H free atoms in the host lattice causes the metal to become more brittle and less resistant to crack formation and propagation. In particular, hydrogen generates an internal stress that lowers the fracture stress of the metal so that brittle crack growth can occur under a hydrogen partial pressure below 1 atm. [43,44].

Some experimental evidence shows that neutron emissions may be strictly correlated to fracture of non-radioactive or inert materials. From this point of view, anomalous nuclear emissions and heat generation had been verified during fracture in fissile materials [2–4] and in deuterated solids [5,8,30]. The experiments recently proposed by Carpinteri et al. [36–39] represent the first evidence of neutron emissions due to piezonuclear fissions observed during failure of inert, stable, and non-radioactive solids under compression, as well as from non-radioactive liquids under ultrasound

cavitation [37,38]. In the present paper, we analyze neutron and alpha particle emissions during tests conducted on an electrolytic cell, where the electrolysis is obtained using Ni–Fe and Co–Cr electrodes in aqueous potassium carbonate solution. Voltage, current intensity, solution conductivity, temperature, alpha and neutron emissions were monitored. The compositions of the electrodes were analyzed both before and after the tests. Strong evidence suggest that so-called Cold Nuclear Fusion, interpreted under the light of hydrogen embrittlement, may be explained by piezonuclear fission reactions occurring in the host metal, instead of by the nuclear fusion of H isotopes adsorbed in the lattice. These new kind of fission reactions have recently been observed from the laboratory to the Earth's crust scale, when particular stress waves originate from fracture or fatigue phenomena, as they do corresponding to an impending earthquake [5–40].

2. Experimental Set-up and Measurement Equipment

2.1. The electrolytic cell and the power circuit

Over the last 10 years, specific experiments have been conducted on an electrolytic reactor (owned by Mr. A. Goi et al.). The aim was to investigate whether the anomalous heat generation may be correlated to new type of nuclear reactions during electrolysis phenomena. The reactor was built in order to be appropriately filled with a salt solution of water and potassium carbonate (K_2CO_3). The electrolytic phenomenon was obtained using two metal electrodes immersed in the aqueous solution. The solution container, named also reaction chamber in the following, is a cylinder-shaped element of 100 mm diameter, with 150 mm high and 5 mm thick. For the reaction chamber, two different materials were used during the experiments: Pyrex glass and Inox AISI 316L steel. The two metallic electrodes were connected to a source

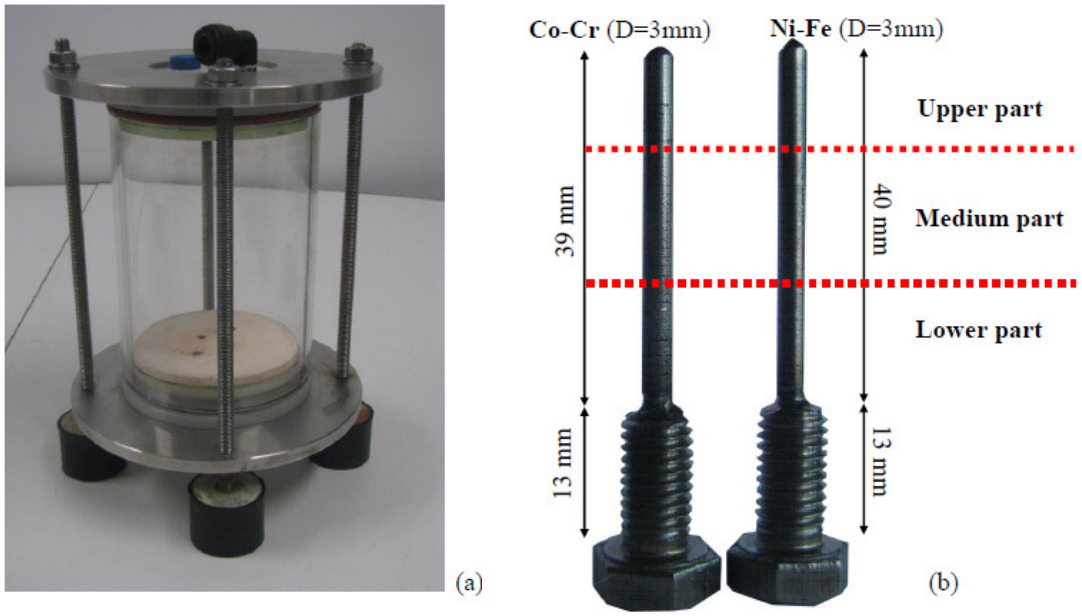

Figure 1. The reaction chamber is a cylinder-shaped element of 100 mm diameter, 150 mm high and 5 mm thick (a). The two electrodes presented a height of about 40 mm of the operating part and a diameter of about 3 mm. The threaded portions and the base are 13 and 5 mm long, respectively (b).

of direct current: an Ni–Fe based electrode as positive pole (anode), and a Co–Cr based electrode as negative pole (cathode) (see Fig. 1b).

With regard to the experiment described in the present paper, after approximately 10 operating hours, the generation of cracks was observed in the glass container, which forced the authors to adopt a more resistant reaction chamber made of steel. Teflon lids are sealed to both the upper and the lower openings of the chamber. The reaction chamber base consists of a ceramic plate preventing the direct contact between liquid solution and Teflon lid (see Fig.1a). Two threaded holes host the electrodes, which are screwed to the bottom of the chamber, which is then filled with the solution. A valve at the top of the cell allows the vapor to escape from the reactor and condense in an external collector. Externally, two circular Inox steel flanges, fastened by means of four threaded ties, hold the Teflon layers. The inferior steel flange of the reactor is connected to four supports isolated from the ground by means of rubber based material. As mentioned before, a direct current passes through the anode and the cathode electrodes, provided by a power circuit connected to the power grid through an electric socket. The components of the circuit are an isolating transformer, an electronic variable transformer (Variac), and a diode bridge linked in series (Fig. 2).

2.2. Measurement equipment and devices

Different physical quantities were measured during the experiments, such as voltage, current, neutron and alpha particle emissions.

Electric current and voltage probes were positioned in different parts of the circuit as it is shown in Fig. 2. The voltage measurements were performed by a differential voltage probe of 100 MHz with a maximum rated voltage of 1400 V. The current was measured by a Fluke I 310S probe with a maximum rated current of 30 A. Particular attention was paid to the data obtained from the current and voltage probes positioned at the input line powering the reaction chamber (probes 7 and 8 in Fig. 2) in order to evaluate the power absorbed by the cell. Current intensity and voltage measurements were also taken by means of a multimeter positioned at the input line. From the turning on to the switching off of the electrolytic cell, current and voltage were found to vary in a range from 3 to 5 A and from 20 to

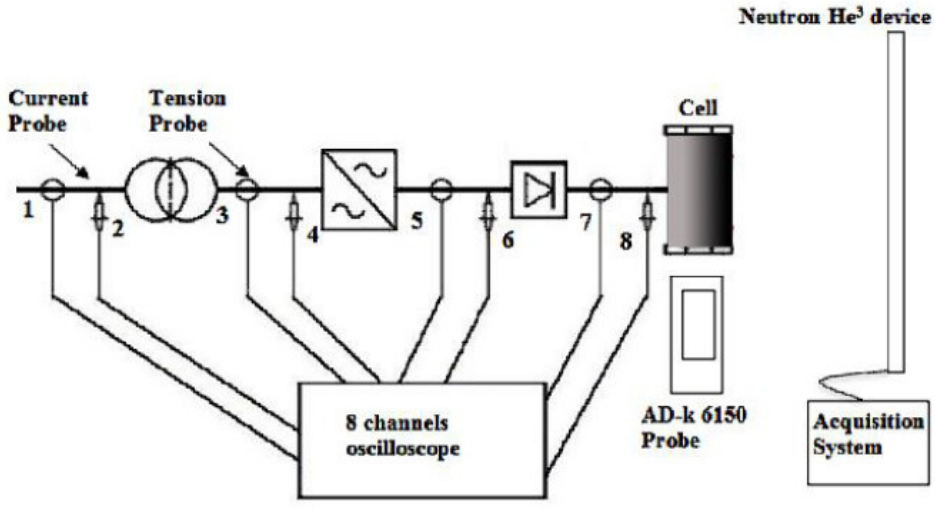

Figure 2. Scheme of the experimental set-up adopted and disposition of the measurement equipment employed during the tests.

120 V, respectively. For convenience and clarity, these values are considered as a benchmark to be compared to further measurements which will be reported in future works.

Regarding the neutron emission measurements, since neutrons are electrically neutral particles, they cannot directly produce ionization in a detector, and therefore cannot be directly detected. This means that neutron detectors must rely upon a conversion process accounting for the interaction between an incident neutron and a nucleus, which produces a secondary charged particle. Such charged particle is then detected and the neutron's presence is revealed from it. For an accurate neutron evaluation a He^3 proportional counter was employed. The detector used in the tests is a He^3 type (Xeram, France) with pre-amplification, amplification, and discrimination electronics directly connected to the detector tube. The detector is supplied by a high voltage power (about 1.3 kV) via NIM (Nuclear Instrument Module). The logic output producing the TTL (transistor–transistor logic) pulses is connected to a NIM counter. The logic output of the detector is enabled for analog signals exceeding 300 mV. This discrimination threshold is a consequence of the sensitivity of the He^3 detector to the gamma rays ensuing neutron emission in ordinary nuclear processes. This value has been determined by measuring the analog signal of the detector by means of a Co-60 gamma source. The detector is also calibrated at the factory for the measurement of thermal neutrons; its sensitivity is 65 cps/$n_{thermal}$ ($\pm 10\%$ declared by the factory), i.e., the flux of thermal neutrons is one thermal neutron/s cm^2, corresponding to a count rate of 65 cps.

For the alpha particle emission, a 6150AD-k probe with a sealed proportional counter was used, which does not require refilling or flushing from external gas reservoirs. The probe is sensitive to alpha, beta, and gamma radiation. An electronic switch allows for the operating mode "alpha" to detect alpha radiation only, such that in this mode the radiation recognition is very sensitive because the background level is much lower. A removable discriminator plate (stainless steel, 1 mm) distinguishes between beta and gamma radiation detection. An adjustable handle can be locked to the most convenient orientation. During the experiments the 6150AD-k probe was used in the operating mode alpha to monitor the background level before and after the switching on of the cell.

Finally, before and after the experiments Energy Dispersive X-ray spectroscopy has been performed in order to recognise possible direct evidence of piezonuclear reactions that can take place during the electrolysis. The elemental analyses were performed by a ZEISS Auriga field emission scanning electron microscope (FESEM) equipped with an Oxford INCA energy-dispersive X-ray detector (EDX) with a resolution of 124 eV @ MnKa. The energy used for the analyses was 18 keV.

3. Experimental Results

3.1. General remarks and preliminary stage

In Fig. 1b, the two electrodes used for the tests are shown. The initial measurement phase implied the use of the Energy Dispersive X-ray spectroscopy (EDX) technique to obtain measurements useful to evaluate the chemical composition of the two electrodes before the experiments. In particular, a series of measures were repeated in three different regions of interest for each electrode in order to obtain a sufficient amount of reliable data. Such regions are the upper, the middle and the lower part of the single electrode, as reported in Fig. 2b.

Table 1. EDX spectroscopy of the K_2CO_3 salt used for the aqueous solution.

Element	Weight%	Atomic%	Compd%	Formula
C	13.02	22.05	47.72	CO_2
K	43.40	22.57	52.28	K_2O
O	43.58	55.38		
Total	100.00			

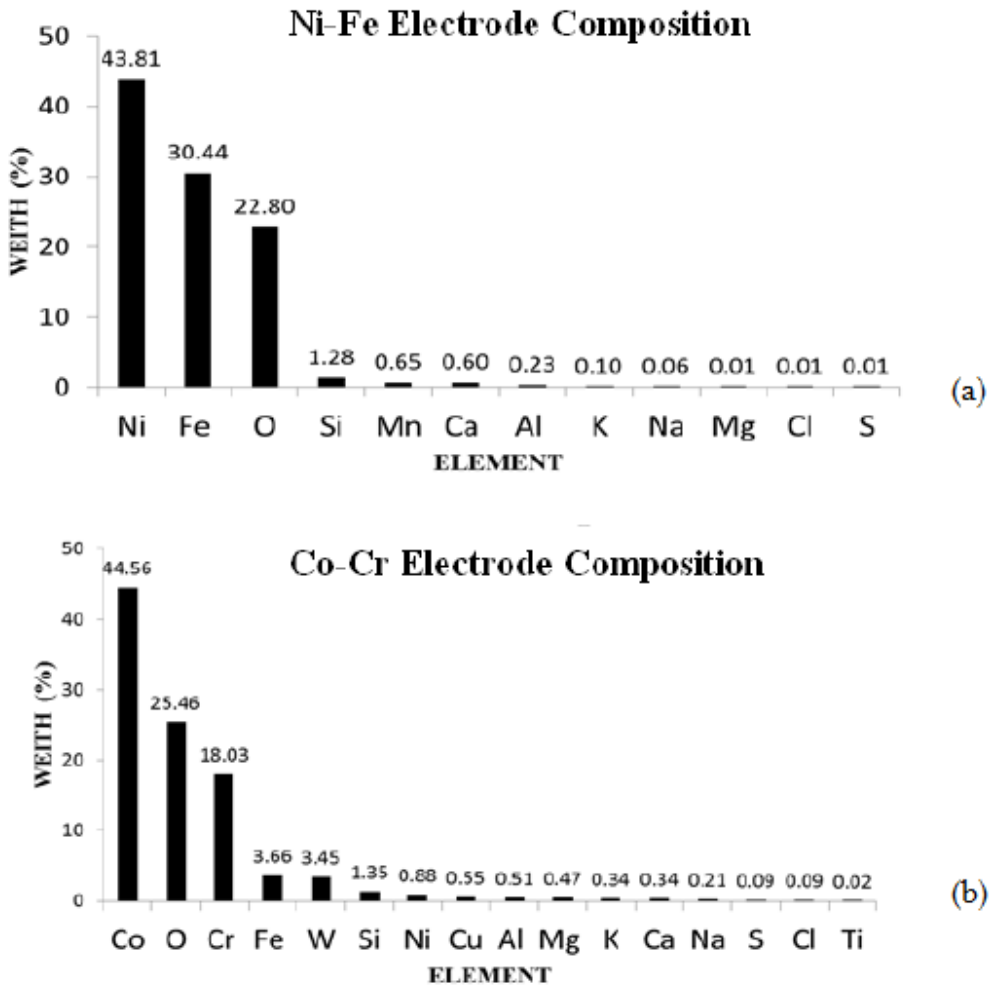

Figure 3. Mean element concentrations of the two electrodes used for the electrolysis.

In Figs. 3a and b, the average element concentrations of the electrodes used for the electrolysis are shown. In the initial condition the Ni–Fe electrode (anode) is composed by approximately 44% in Ni, 30% in Fe, and 23% in O. The remaining percentage includes contents of Si, Mn, Ca, Al, K, Na, Mg, Cl, and S, observable only in traces (Fig. 3a). On the other hand, the Co–Cr cathode is composed approximately by 44% in Co, 18% in Cr, 4% in Fe, 25% in O, and traces of other elements such as Si, Al, Mg, Na, W, Cu, and S (Fig. 3b). Table 1 summarizes the results for the compositional

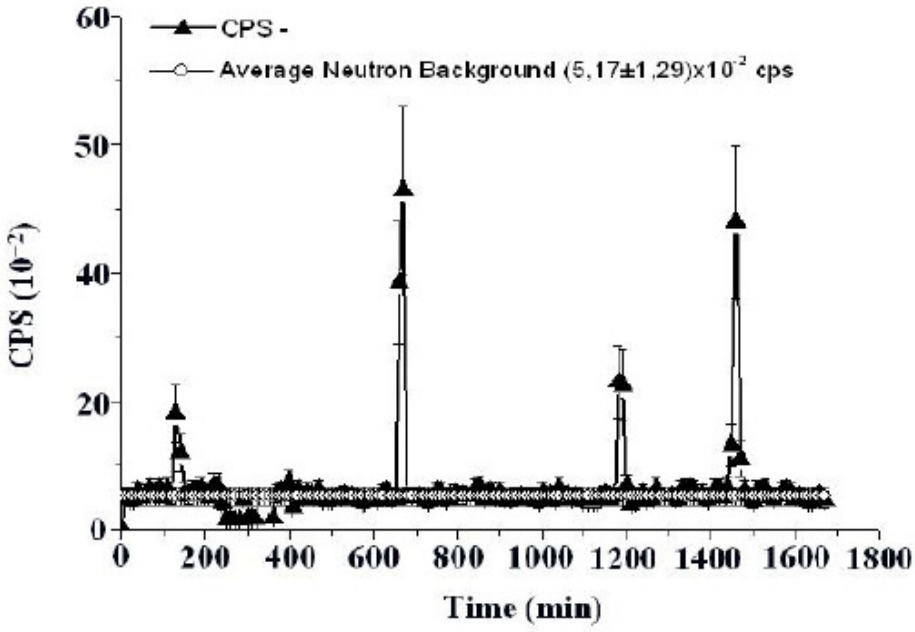

Figure 4. Neutron emission measurements. emissions between 4 and 10 times the background level have been observed during the experiments.

analysis conducted on the K_2CO_3, the salt used for the aqueous solution (K_2CO_3+H_2O), where the solute to solvent ratio was approximately 40 g/l.

3.2. Neutron and alpha particle detection during the experiment

Neutron emission measurements performed during the experimental activity are represented in Fig. 4. The measurements performed by the He^3 detector were conducted for a total time of about 26 h. The background level was measured for different time spans before and after switching on the reaction chamber. These measurements reported an average neutron background of $(5.17 \pm 1.29) \times 10^{-2}$ cps. Furthermore, when the reactor is active, it is possible to observe that after a time span of more than 3 h (200 min) neutron emissions of about four times the background level may be observed. After less than 11 h (650 min) from the beginning of the measurements, it is possible to observe a neutron emission level of about one order of magnitude greater than the background level. Similar results were observed after 20 h (1200 min) and 25 h (1500 min) when neutron emissions of about 5 times and 10 times the background were measured, respectively.

In Figs. 5a and b, alpha particle emissions are shown. The data are related to an alpha emission level monitored by means of the 6150AD-k probe set to the operating mode "alpha". The measurements shown in Fig. 5a are referred to the data acquired for a time interval equal to 60 minutes when the reaction chamber was operating (cell on). The data in Fig. 5b represent the alpha particle emissions corresponding to the background level and are obtained by measurements acquired, also in this case, for a 60 min (cell off) time interval. From these figures, it can be noticed that the number of counts per second acquired by the probe increased considerably when the electrolytic cell was operating (cell on) (Fig. 5a). In addition, the mean values of two alpha emission time series were computed, one when the cell was switched

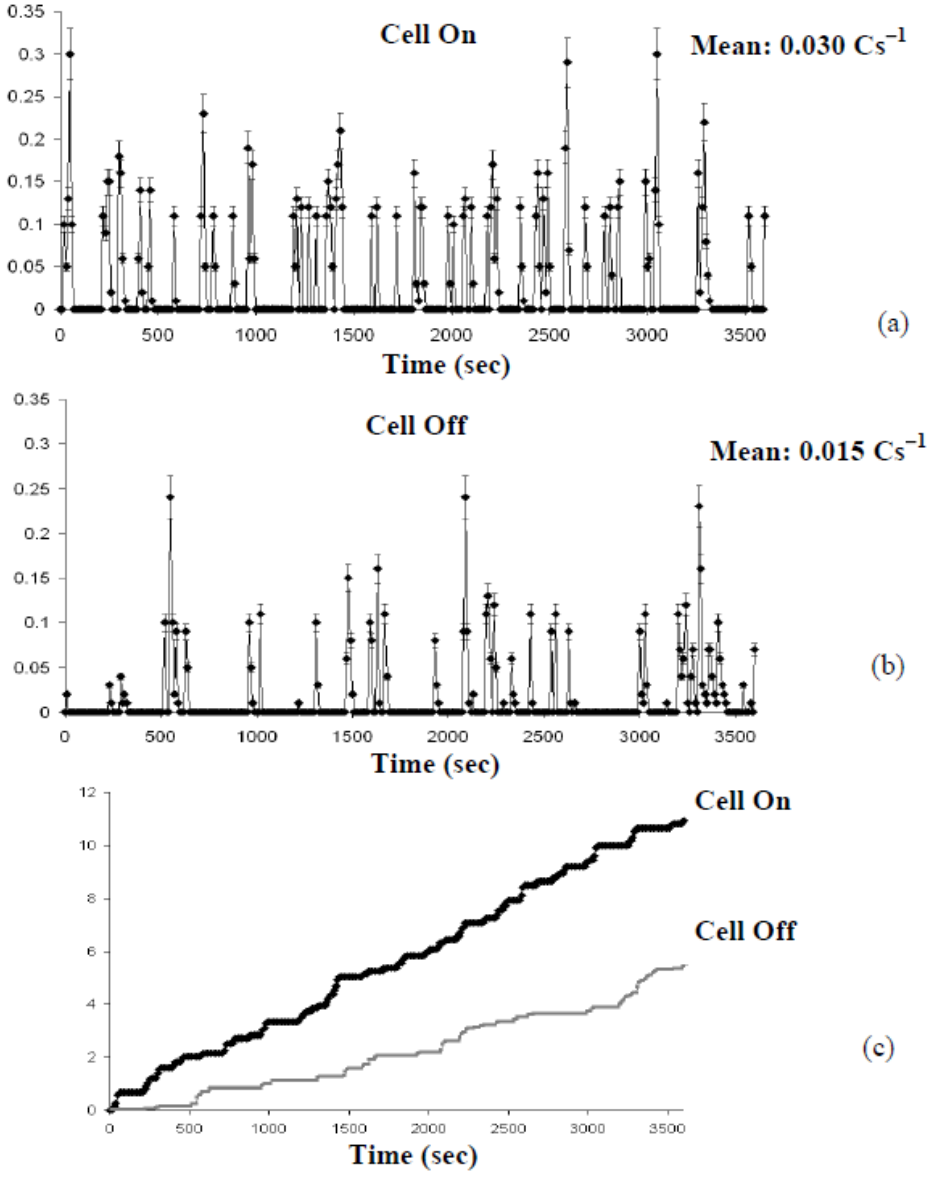

Figure 5. Data acquired for a time interval equal to 60 min when the reaction chamber was operating (a). The alpha particle emissions corresponding to the background level (b). Cumulative curves for the alpha emissions (c).

on and the other when the cell was off. The first time series, showed an average alpha emission of about 0.030 c/s (count per second), whereas the second one provided the background emission level in the laboratory with a mean

value of about 0.015 c/s. It is evident that the average alpha particle emission during the electrolysis is two times the background level. These results, together with the evidence of neutron emissions reported in Fig. 4, are particularly interesting when considering the compositional variation described in the following, and will be useful to corroborate the hypothesis of piezonuclear fission for the chemical elements constituting the electrodes. In Fig. 5c, the cumulative curves for the alpha emission counts are reported. It is evident that the total counts value, monitored when the cell was operating (cell on), is approximately twice the value measured for the background level (cell off).

3.3. Compositional analysis of the electrodes

As reported in the previous section, Energy Dispersive X-ray Spectroscopy was performed in order to recognise possible direct evidence of piezonuclear reactions taking place during the electrolysis. In Figs. 6a and b two images of the Co–Cr electrode surface respectively before the experiment and after 32 h from the beginning of it are reported. It is shown that the electrode after several operating hours presented micro-cracks and cracks visible on its external surface (see Fig. 6b).

The experimental activity was developed in three different phases in order to investigate possible compositional variations on the electrode surface. A first analysis was carried out to evaluate the composition of the electrodes before they underwent the electrolysis experiment (0 h) (see Table2). The second analysis was conducted after an initial operating time of the electrolytic cell of about 4 h (see Table 2). After this, a third and a fourth step analyses were performed. For these two steps, the cell operated for 28 and 6 h, respectively, corresponding to a cumulative working time of 32 (4 h+28 h) and 38 h (4 h+28 h+6 h) (see Table2). In the case of the Ni–Fe electrode, the resulting mean concentrations of Ni, Si, Mg, Fe, and Cr are reported for each step, see Table 2. In Figs. 7–11, the EDX measurements for each element are reported considering the four steps previously mentioned (Figs. 7a, 8a, 9a, 10a, and 11a). At the same time, the evolution of the mean values of each time series along with their respective standard deviations, corresponding to 0, 4, 32, and 38 h, are reported by histograms (Figs. 7b, 8b, 9b, 10b, and 11b). After 38 h, the appearance of Cr, before absent, was detected as reported in Table 2 and in Fig. 11a. In particular, the Ni concentration showed a total average decrease of 8.6% from 43.9% to 35.3% after 38 h (see Table 2 and Figs. 7a and b). This Ni depletion is one fourth of the initial Ni concentration. A mean increment in Si concentration after 32 h of 3.9% and an average increment in Mg concentration after 38 h, starting from 0.1% up to 4.8%, can be observed from the data reported in Table 2, Figs. 8 and 9. Similar considerations may be done also for Fe and Cr concentrations. The average Fe content decreased of 3.2%, changing from 30.5% to 27.3% at the end of the experiment (see Table 2 and Fig. 10). On the other hand, the Cr concentration appeared only in the last phase with an appreciable increase of 3.0% (see Table 2 and Fig. 11). Such decreases in Ni and Fe seem to be almost perfectly counterbalanced by the increases in other elements: Si, Mg, and Cr. In particular, since the analysis excluded Ni content variations on the other electrode, the balance: Ni (–8.6%) = Si (+3.9%) + Mg (+4.7%) can be reasonably explained only by the following symmetrical piezonuclear fissions:

$$\mathrm{Ni}_{28}^{59} \rightarrow \ 2\mathrm{Si}_{14}^{28} + 3 \text{ neutrons}, \tag{1}$$

Table 2. Ni–Fe Electrode, Element concentration before the experiment, after 4, 32 and 38 h of the test. The values reported for the mass % of each element are referred as the mean value of all the effectuated measurements.

	Ni (%)	Si (%)	Mg (%)	Fe (%)	Cr (%)
Before the experiment	43.9	1.1	0.1	30.5	–
After 4 h	43.6	1.1	0.4	30.7	–
After 32 h	35.2	5.0	0.2	27.9	–
After 38 h	35.3	1.5	4.8	27.3	3.0

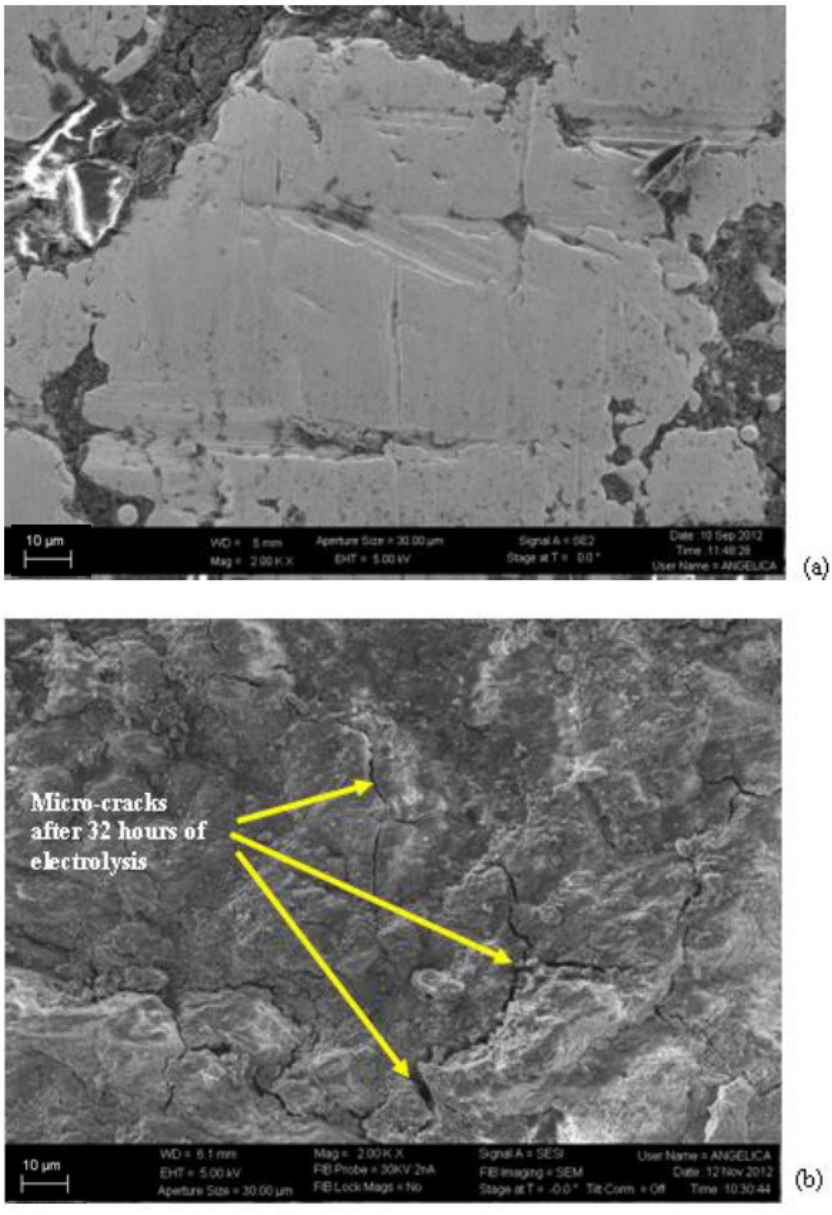

Figure 6. Image of the Co–Cr electrode surface before the experiment (a). The electrode after many operating hours presented cracks and micro-cracks visible on the external surfaces (b).

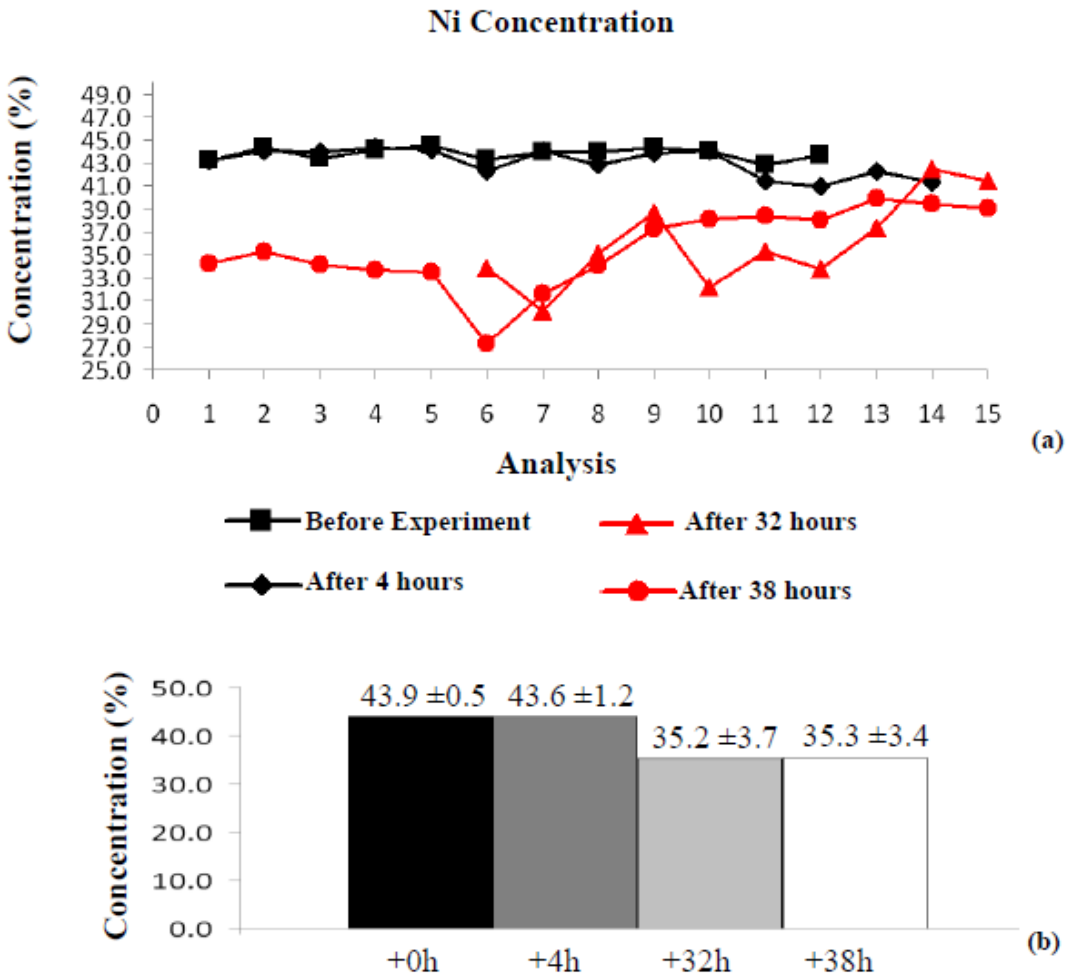

Figure 7. Ni concentration before the experiment, after 4, 32 and 38 h (a). The average values of Ni concentration change from a mass percentage of 43.9% at the beginning of the experiment to 35.2 and 35.3% after 32 and 38 h, respectively (b).

$$Ni_{28}^{59} \rightarrow \ 2Mg_{12}^{24} + 2He_{2}^{4} + 3 \text{ neutrons}. \tag{2}$$

At the same time, the balance Fe (–3.2%) ≅ Cr (+3.0%) may be explained by the reaction:

$$Fe_{26}^{56} \rightarrow \ Cr_{24}^{52} + He_{2}^{4}\ . \tag{3}$$

It is very interesting to notice that reactions (1) and (2) imply neutron emissions, as well as reactions (2) and (3) imply the emissions of alpha particles.

As far as the Co–Cr electrode is concerned, it is possible to observe variations even more evident in the concentrations of the most abundant constituting elements. In particular, the average Co concentration decreased by 23.5%, from an

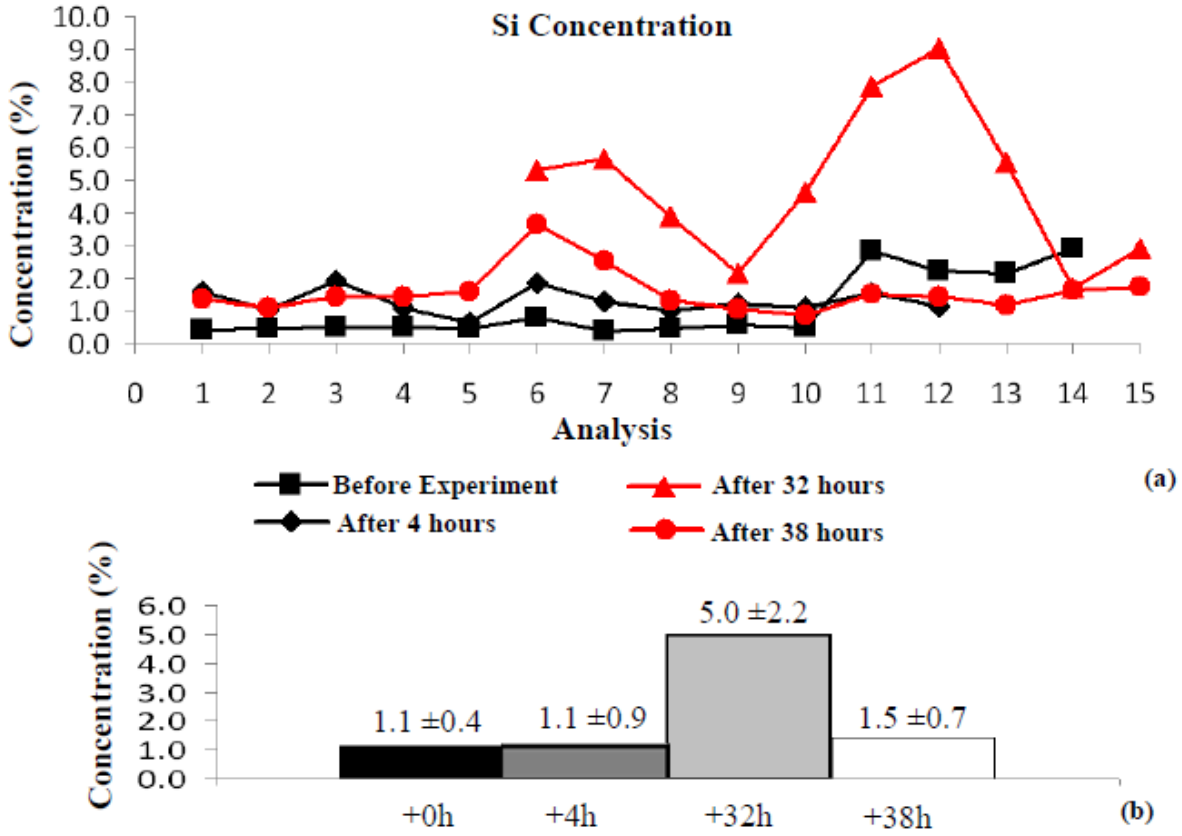

Figure 8. Si concentration before the experiment, after 4, 32 and 38 h (a). The mean values of Si concentration change from a mass percentage of 1.1% at the beginning of the experiment to 5.0 and 1.5% after 32 and 38 h, respectively (b).

initial percentage of 44.1% to a concentration of 20.6% after 32 h (see Table 3 and Figs. 12a and b). At the same time an increment of 23.2% can be observed in the Fe content after 32 h, changing from 3.1% before the experiment to 26.3% at the end of the second phase (see Table 3 and Figs. 13a and b). It is rather impressive that the decrease in Co and the increase in Fe are almost the same: Co (–23.5%) ≅ Fe (+23.2%). According to the compositional analysis on the Ni–Fe electrode no Co concentration was found that could lead us to consider the chemical migration to explain its depletion in the Co–Cr electrode, thus the following reaction seems the most reasonable possibility:

$$Co_{27}^{59} \rightarrow Fe_{26}^{56} + H_1^1 + 2 \text{ neutrons}. \quad (4)$$

In Table 3 and in Figs. 14 and 15, Cr and K concentrations are reported for the different phases of the experiment. The K increase by about 12.4% after 32 h may be only partially counterbalanced by the decrease in Cr (8.1%) according to reaction (5). The remaining increment of K (4.3%) could be considered as an effect of the K_2CO_3 aqueous solution deposition at the end of the third step.

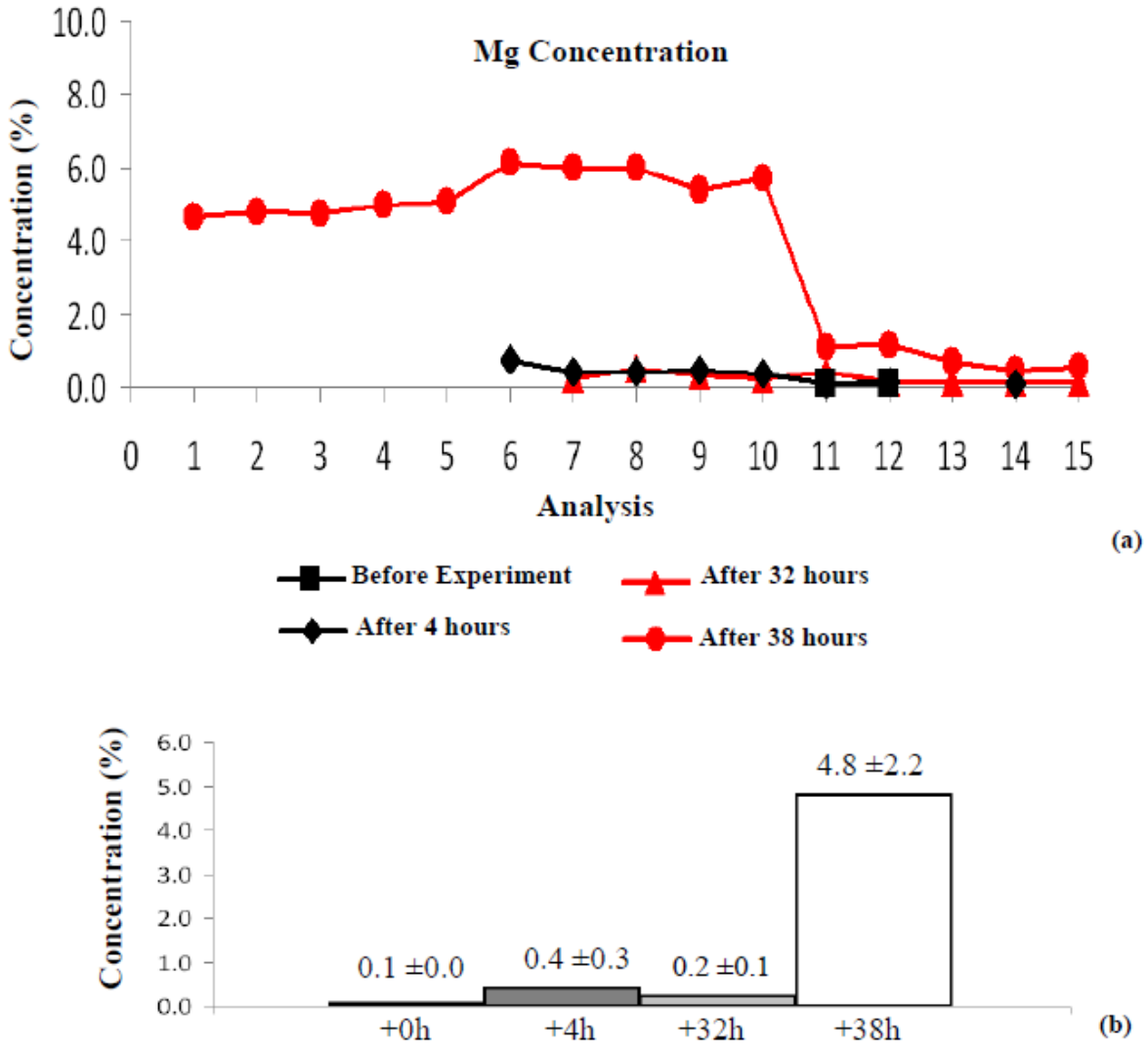

Figure 9. Mg concentration before the experiment, after 4, 32 and 38 h (a). The mean values of Mg concentration change from a mass percentage of 0.1% and 0.4% at the beginning of the experiment to 4.8% after 38 h (b).

Considering these variations also the following piezonuclear reaction, involving Cr as the starting element and K as the resultant could be considered:

$$Cr_{24}^{52} \rightarrow K_{19}^{39} + He_{1}^{1} + 2He_{2}^{4} + 4 \text{ neutrons}. \quad (5)$$

Also in this case, it is remarkable that both reactions (4) and (5) imply neutron emissions, while reaction (5) implies also the emission of alpha particles.

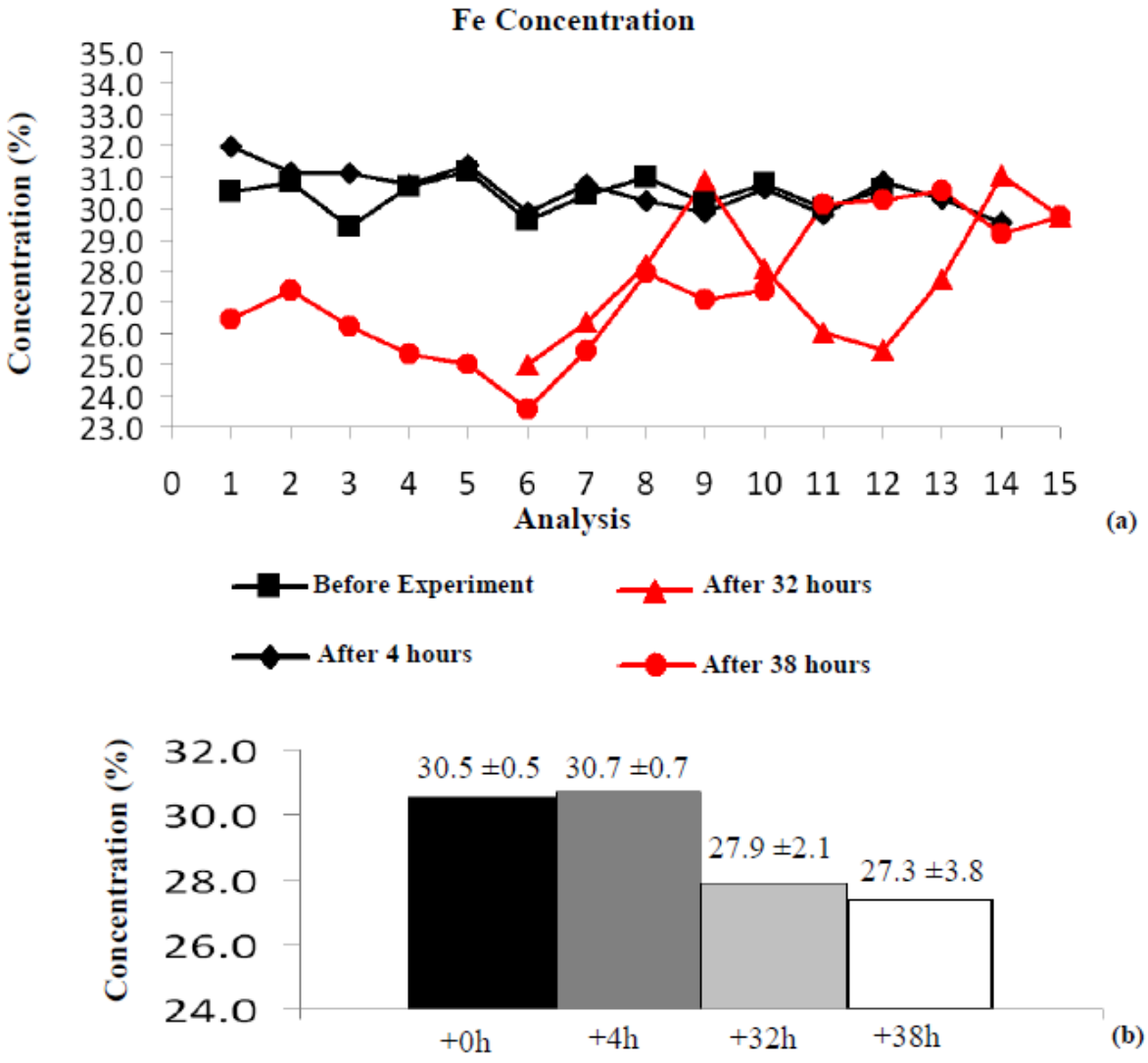

Figure 10. Fe concentration before the experiment, after 4, 32 and 38 h (a). The mean values of Fe concentration change from a mass percentage of 30.5% at the beginning of the experiment to 27.9% and 27.3% after 32 and 38 h, respectively (b).

It is important to consider that the balances reported, for Ni–Fe electrode (reactions (1)–(3)) and for Co–Cr electrode (reactions (4), (5)), were obtained considering the values of the second or third step corresponding to the larger variation for each element concentration (see Tables 2 and 3). Additional variations observed for some of these elements, such as Si, Co and Fe, between the second and the third step, may be explained considering other possible secondary piezonuclear reactions occurring on the electrode surface. Further efforts should be devoted to evaluate the evidence of these secondary fissions.

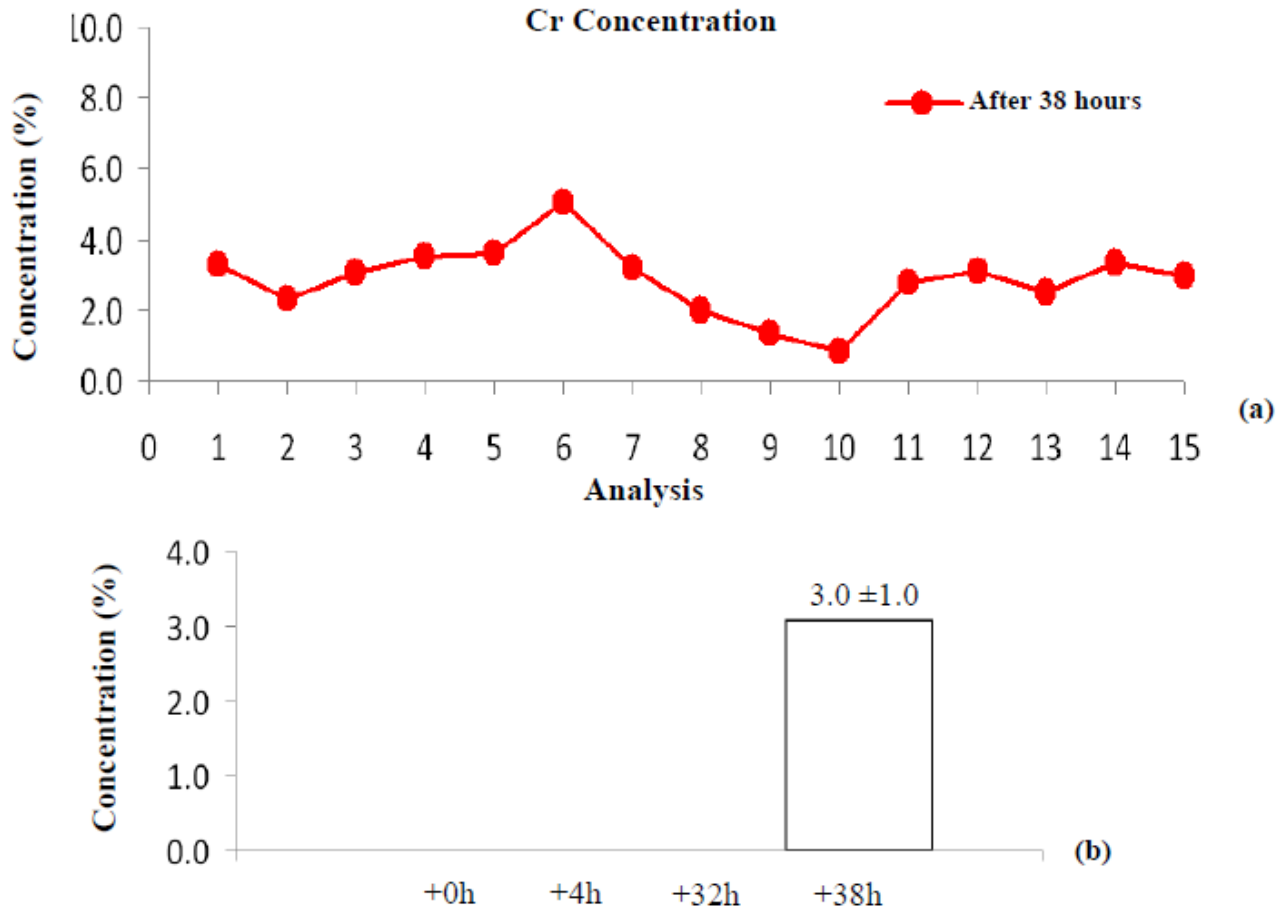

Figure 11. Cr concentration after 38 h (a). The mean value of Cr concentration changes from 0 % (absence of this element) to a mass percentage of 3.0% after 38 h (b).

All these results suggest that during gas loading, performed with hydrogen or deuterium, the host lattice is subjected to mechanical damaging and fracturing due to atoms absorption and penetration. Evidence of diffused cracking was identified also on the electrode surface after the experiments (see Fig. 6b). Based on this, we argue that the hydrogen, favoring the crack formation and propagation in the metal, comes from the electrolysis of water. In fact, because the electrodes immersed in a liquid solution, their surface is exposed to the formation of gaseous hydrogen due to the decomposition of water caused by the current passage.

4. Conclusions

Neutron emissions up to one order of magnitude higher than the background level were observed during the operating time of an electrolytic cell. In particular, after a time span of about 3 h, neutron emissions of about four times the

Table 3. Co–Cr Electrode, Element concentration before the experiment, after 4, after 32 and 38 h of the test. The values reported for the mass % of each element are referred as the mean value of all the effectuated measurements.

	Co(%)	Fe(%)	Cr(%)	K(%)
Before the experiment:	44.1	3.1	17.8	0.5
After 4 h	43.7	1.6	17.8	2.2
After 32 h	20.6	26.3	9.7	12.9
After 38 h	34.4	6.6	5.1	4.4

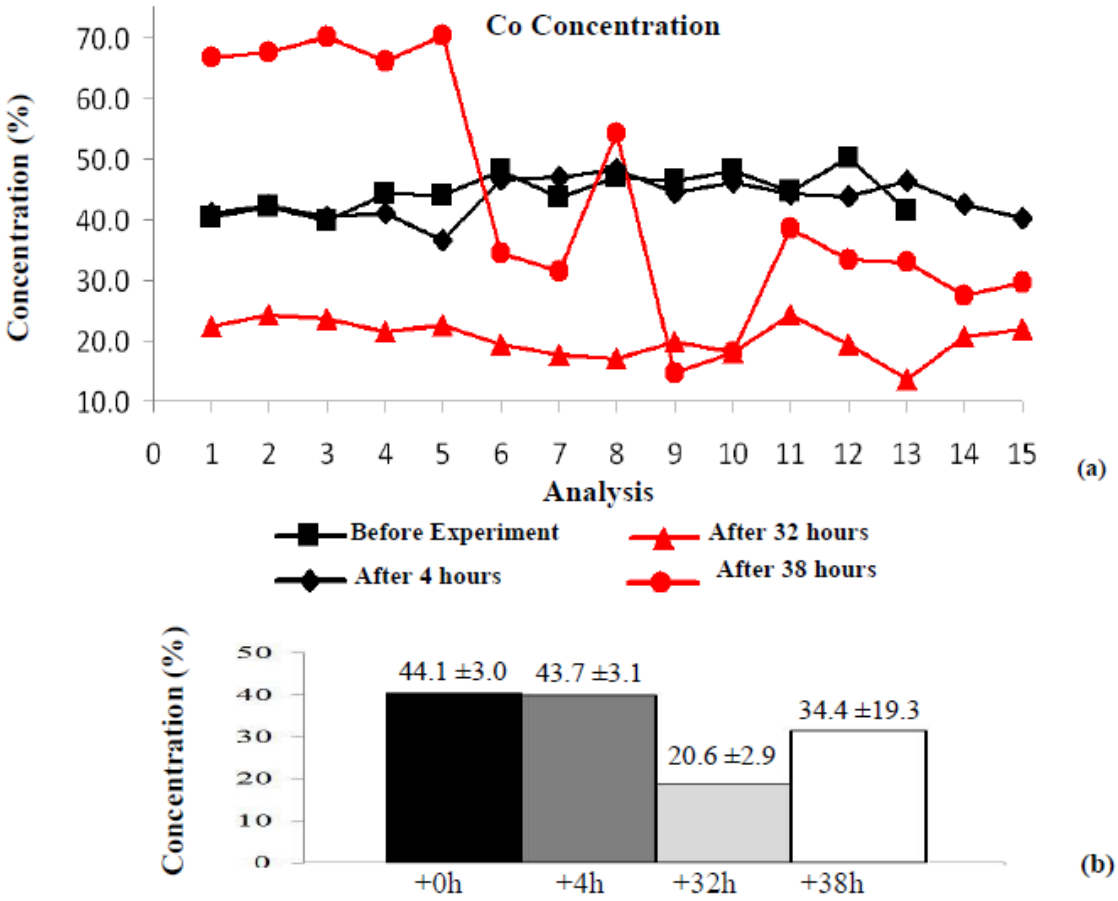

Figure 12. Co concentration before the experiment, after 4, 32 and 38 h (a). The mean values of Co concentration change from a mass percentage of 44.1% at the beginning of the experiment to 20.6 and 34.4% after 32 and 38 h, respectively (b).

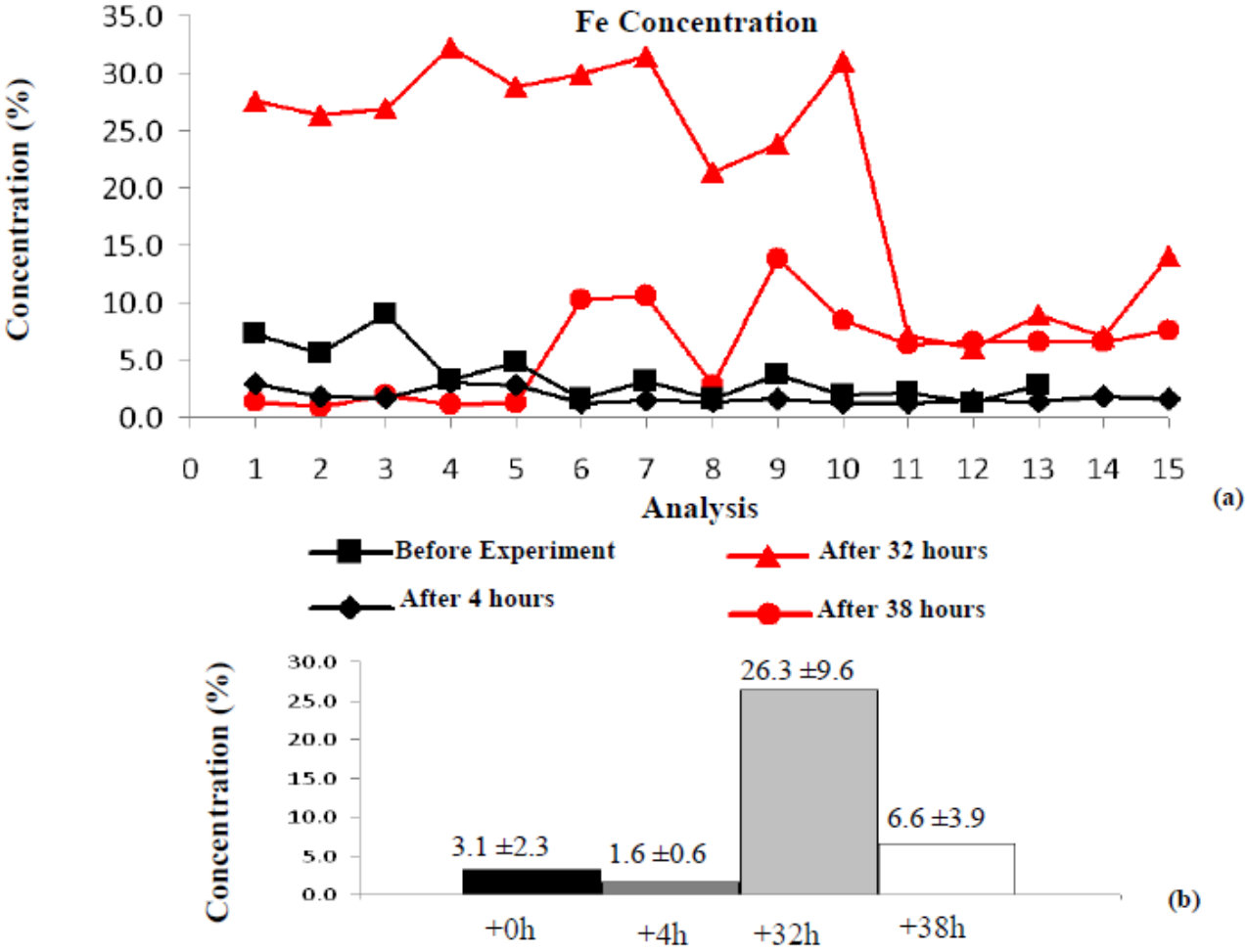

Figure 13. Fe concentration before the experiment after 4, 32 and 38 h (a). The mean values of Fe concentration change from a mass percentage of 3.1% at the beginning of the experiment to 26.3 and 6.6% after 32 and 38 h, respectively (b).

background level were measured. After 11 h, it was possible to observe neutron emissions of about one order of magnitude greater than the background level. Similar results were observed after 20 and 25 h.

When the cell was switched on, the average alpha particle emission was about 0.030 c/s for 1 h of measurement; this value corresponds to an alpha emission level of about two times the background measured in the laboratory before and after the experiment (0.015 c/s).

By the EDX analysis performed on the two electrodes in three successive steps, significant compositional variations could be recorded. In general, the decreases in Ni and Fe in the Ni–Fe electrode seem to be almost perfectly counterbalanced by the increases in lighter elements: Si, Mg, and Cr. In fact, the balance Ni (–8.6%) ≅ Si (+3.9%) + Mg

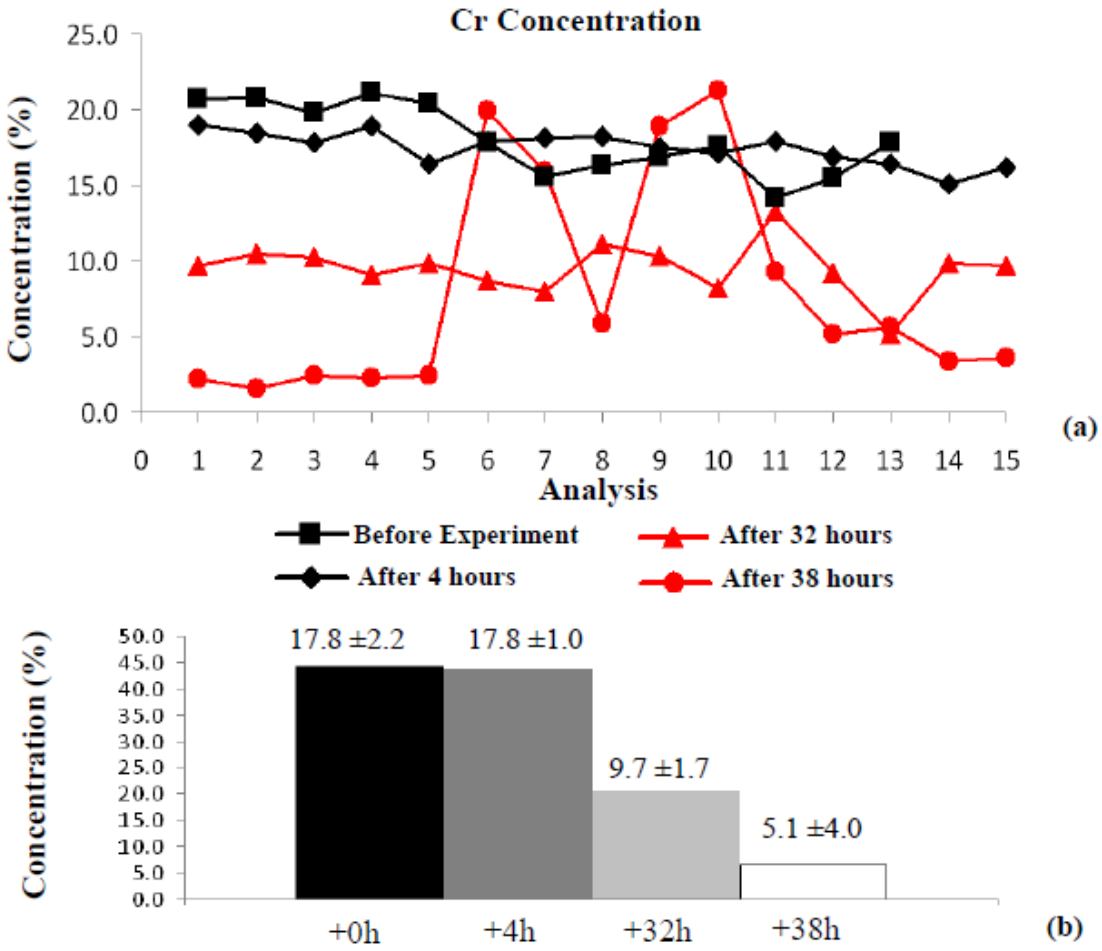

Figure 14. Cr concentration before the experiment after 4, 32 and 38 h (a). The Cr concentration changes from a mass percentage of 17.8% to 9.7% and 5.1% after 32 and 38 h (b).

(+4.7%) is satisfied by reactions (1) and (2). Specifically, Si could have also undergone further reactions, which would explain its drop in concentration observed at the third step. At the same time, the balance Fe (–3.2%) ≅ Cr (+3.0%) may be explained considering reaction (3).

As far as the Co–Cr electrode is concerned, the Co decrease is almost perfectly counterbalanced by the Fe increase: Co (–23.5%) ≅ Fe (+23.2%). This last evidence, which is really impressive considering the mass percentage involved, seems to be explainable only considering reaction (4). Finally, the Cr decrease and the K increase may be explained taking into account reaction (5) and the solution deposition. In particular, the K increase by about 12.4% may be only partially counterbalanced by the decrease in Cr (8.1%) according to reaction (5). The remaining increment in K (4.3%) could be considered as an effect of the K_2CO_3 aqueous solution deposition at the end of the third step.

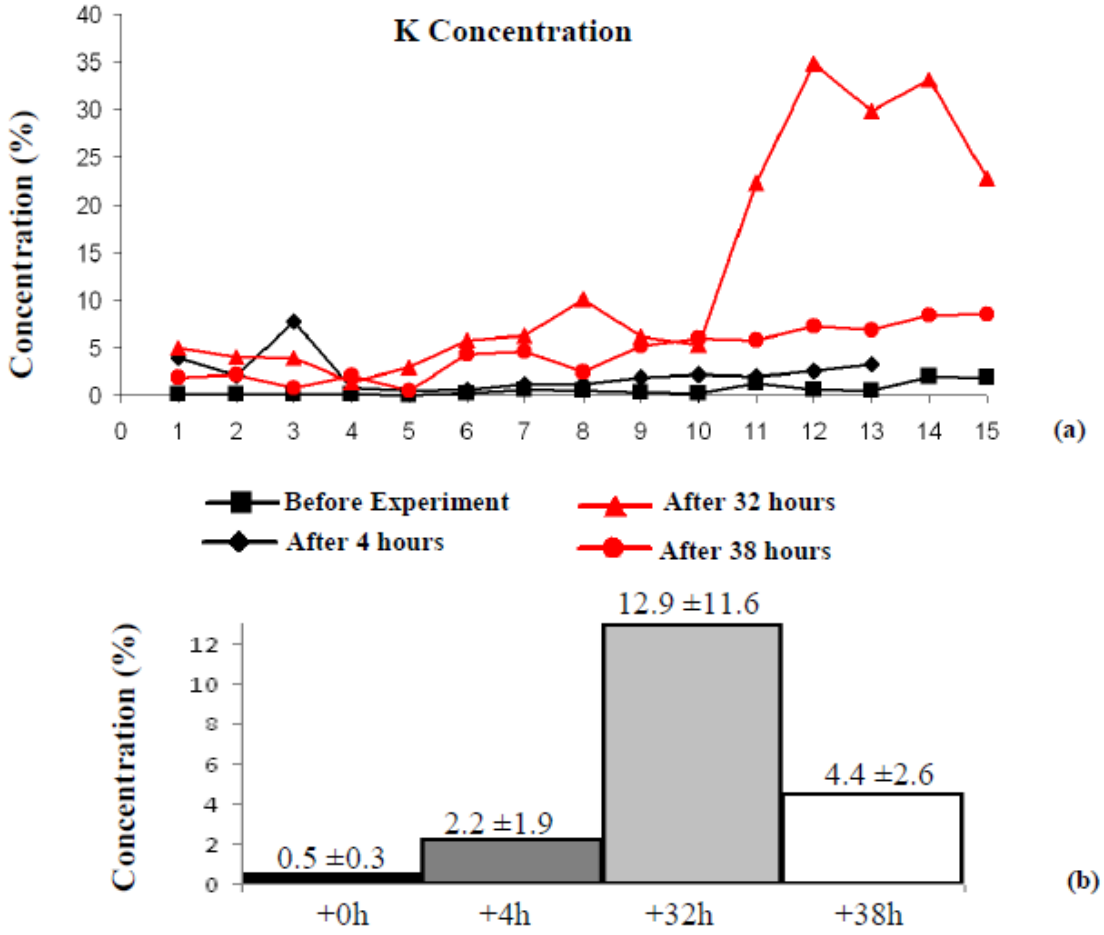

Figure 15. K concentration before the experiment after 4, 32 and 38 h (a). The K concentration changes from 0.5 and 2.2% after 4 h to 12.9 and 4.4% after 32 and 38 h (b).

Chemical variations and energy emissions may be accounted for direct and indirect evidence of mechano-nuclear fission reactions correlated to micro-crack formation and propagation due to hydrogen embrittlement. According to this interpretation of so-called Cold Nuclear Fusion, hydrogen, which is imputed to favor the crack formation and propagation in the electrodes, comes from the electrolysis of water. Being the electrodes immersed in a liquid solution, the metal surface is exposed to the formation of gaseous hydrogen due to the decomposition of water molecule caused by the current passage. In addition, the high current density contributes to the formation and penetration of hydrogen into the metal. So-called Cold Nuclear Fusion, interpreted under the light of hydrogen embrittlement, may be explained by piezonuclear fission reactions occurring in the host metal, rather than by nuclear fusion of hydrogen isotopes forced into the metal lattice.

Aknowledgements

Dr. A. Sardi and Dr. F. Durbiano are gratefully acknowledged for their help during the experimental set-up definition and for the assistance given during the measurements. Also Dr. A. Chiodoni is warmly acknowledged for the EDX spectroscopy analyses.

References

[1] Borghi, D.C. Giori, D.C. Dall'Olio, A., *Experimental Evidence for the Emission of Neutrons from Cold Hydrogen Plasma*, CEN, Recife, Brazil, 1957.
[2] Diebner, K., Fusionsprozesse mit Hilfe konvergenter Stosswellen – einige aeltere und neuere Versuche und Ueberlegungen, *Kerntechnik.* **3** (1962) 89–93.
[3] Kaliski, S., Bi-conical system of concentric explosive compression of D—T, *J. Tech. Phys.* **19** (1978) 283–289.
[4] Winterberg, F., Autocatalytic fusion–fission implosions, *Atomenergie-Kerntechnik* **44** (1984) 146.
[5] Derjaguin, B. V. et al., Titanium fracture yields neutrons? *Nature* **34** (1989) 492.
[6] Fleischmann, M. Pons S. and Hawkins M., Electrochemically induced nuclear fusion of deuterium, *J. Electroanal. Chem.* **261** (1989) 301.
[7] Bockris, J.O'M. Lin, G.H. Kainthla, R.C. Packham, N.J.C. and Velev, O., Does Tritium Form at Electrodes by Nuclear Reactions? *The First Annual Conference on Cold Fusion*. National Cold Fusion Institute, University of Utah Research Park, Salt Lake City, 1990.
[8] Preparata, G., Some theories of cold fusion: A review, *Fusion Technol.* **20** (1991) 82.
[9] Preparata, G., A new look at solid-state fractures, particle emissions and "cold" nuclear fusion, *Il Nuovo Cimento* **104A** (1991) 1259–1263.
[10] Mills, R.L. and Kneizys, P., Excess heat production by the electrolysis of an aqueous potassium carbonate electrolyte and the implications for cold fusion, *Fusion Technol.* **20** (1991) 65.
[11] Notoya, R. and Enyo, M., Excess heat production during electrolysis of H_2O on Ni, Au, Ag and Sn electrodes in alkaline media, *Proc. Third Int. Conf. on Cold Fusion*, Nagoya Japan, Universal Academy Press, Tokyo, Japan, 1992.
[12] Miles, M.H. Hollins, R.A. Bush, B.F. Lagowski, J.J. and Miles, R.E., Correlation of excess power and helium production during D_2O and H_2O electrolysis using palladium cathodes, *J. Electroanal. Chem.* **346** (1993) 99–117.
[13] Bush, R.T. and Eagleton, R.D., Calorimetric studies for several light water electrolytic cells with nickel fibrex cathodes and electrolytes with alkali salts of potassium, rubidium, and cesium, *Fourth Int. Conf. on Cold Fusion,* Lahaina, Maui. Electric Power Research Institute 3412 Hillview Ave., Palo Alto, CA 94304, 1993, p. 13.
[14] Fleischmann, M. Pons, S. Preparata, G., Possible theories of cold fusion, *Nuovo Cimento Soc. Ital. Fis. A* **107** (1994) 143.
[15] Szpak, S. Mosier-Boss, P.A. and Smith, J.J., Deuterium uptake during Pd–D codeposition, *J. Electroanal. Chem.* **379** (1994) 121.
[16] Sundaresan, R. and Bockris, J.O.M., Anomalous reactions during arcing between carbon rods in water, *Fusion Technol.* **26** (1994) 261.
[17] Arata, Y., Zhang, Y., Achievement of solid-state plasma fusion ("cold-fusion"), *Proc. Jpn Acad.* Ser. B **71** (1995) 304–309.
[18] Ohmori, T. Mizuno, T. and Enyo, M., Isotopic distributions of heavy metal elements produced during the light water electrolysis on gold electrodes, *J. New Energy* **1**(3) (1996) 90.
[19] Monti, R.A., Low energy nuclear reactions: Experimental evidence for the alpha extended model of the atom, *J. New Energy* **1**(3) (1996) 131.
[20] Monti, R.A., Nuclear transmutation processes of lead, silver, thorium, uranium, *The Seventh Int. Conf. on Cold Fusion*, ENECO Inc., Vancouver, Canada, Salt Lake City, UT, 1998.
[21] Ohmori, T. Mizuno T., Strong excess energy evolution, new element production, and electromagnetic wave and/or neutron emission in light water electrolysis with a tungsten cathode, *Infinite Energy* Issue **20** (1998) 14–17.
[22] Mizuno, T., Nuclear transmutation: the reality of cold fusion, Infinite Energy Press, 1998.
[23] Little, S.R. Puthoff, H.E. and Little, M.E., Search for excess heat from a Pt electrode discharge in K_2CO_3–H_2O and K_2CO_3–D_2O electrolytes, September (1998).

[24] Ohmori, T. and Mizuno, T., Nuclear transmutation reaction caused by light water electrolysis on tungsten cathode under incandescent conditions, *Infinite Energy* **5**(27) (1999) 34.
[25] Ransford, H.E., Non-stellar nucleosynthesis: transition metal production by DC plasma-discharge electrolysis using carbon electrodes in a non-metallic cell, *Infinite Energy* **4** (23) (1999) 16.
[26] Storms, E., Excess power production from platinum cathodes using the Pons–Fleischmann effect, *8th Int. Conf. on Cold Fusion*, Lerici (La Spezia), Italian Physical Society, Bologna, Italy, 2000, pp. 55–61.
[27] Storms, E., *Science of Low Energy Nuclear Reaction: A Comprehensive Compilation of Evidence and Explanations About Cold Fusion*, World Scientific, Singapore, 2007.
[28] Mizuno, T. et al., Production of heat during plasma electrolysis, *Jpn. J. Appl. Phys. A* **39** (2000) 6055.
[29] Warner, J. Dash, J. and Frantz. S., Electrolysis of D_2O with titanium cathodes: enhancement of excess heat and further evidence of possible transmutation, *The Ninth Int. Conf. on Cold Fusion,* Tsinghua University, Beijing, China, 2002, p. 404.
[30] Fujii, M. F. et al., Neutron emission from fracture of piezoelectric materials in deuterium atmosphere, *Jpn. J. Appl. Phys.* **41** (2002) 2115–2119.
[31] Mosier-Boss, P.A. et al., Use of CR-39 in Pd/D co-deposition experiments, *Eur. Phys. J. Appl. Phys.* **40** (2007) 293–303.
[32] Swartz, M., Three physical regions of anomalous activity in deuterated palladium, *Infinite Energy* **14** (2008) 19–31.
[33] Mosier-Boss, P.A., et al., Comparison of Pd/D co-deposition and DT neutron generated triple tracks observed in CR-39 detectors, *Eur. Phys. J. Appl. Phys.* **51**(2) (2010) 20901–20911.
[34] Kanarev, M. Mizuno, T., Cold fusion by plasma electrolysis of water, *New Energy Technol.* **1** (2002) 5–10.
[35] Cardone, F. Mignani, R., *Energy and Geometry*, World Scientific, Singapore, Chapter 10, 2004.
[36] Carpinteri, A. Cardone, F. Lacidogna, G., Piezonuclear neutrons from brittle fracture: Early results of mechanical compression tests, *Strain* **45** (2009) 332–339. *Atti dell'Accademia delle Scienze di Torino* **33** (2009) 27–42.
[37] Cardone, F., Carpinteri, A., Lacidogna G., Piezonuclear neutrons from fracturing of inert solids, *Phys. Lett. A*. **373** (2009) 4158-4163.
[38] Carpinteri, A. Cardone, F. Lacidogna G., Energy emissions from failure phenomena: Mechanical, electromagnetic, nuclear, *Experimental Mechanics* **50** (2010) 1235-1243.
[39] Carpinteri, A., Lacidogna, G., Manuello, A., Borla O., Piezonuclear fission reactions: evidences from microchemical analysis, neutron emission, and geological transformation, *Rock Mechanics and Rock Eng.* **45** (2012) 445–459.
[40] Carpinteri, A., Lacidogna, G., Manuello, A.,. Borla O., Piezonuclear fission reactions from earthquakes and brittle rocks failure: Evidence of neutron emission and nonradioactive product elements, *Experimental Mechanics* **53** (2013) 345–365.
[41] Widom, A., Swain, J., Srivastava, Y.N., Photo-disintegratin of the Iron Nucleus in Fractured Magnetite Rocks with Magetostriction, arXiv: 1306.6286v1 (2013).
[42] Widom, A., Swain, J., Srivastava, Y.N., Neutron production from the fracture of piezoelectric rocks, *J. Phys. G: Nucl. Part. Phys.* **40** (2013) doi:10.1088/0954-3899/40/1/015006.
[43] Milne, I. Ritchie, R.O. Karihaloo, B., *Comprehensive Structural Integrity: Fracture Of Materials From Nano To Macro*, Vol. 6, Chapter 6.02, Elsevier, Amsterdam, 2003, pp. 31–33.
[44] Liebowitz, H., *Fracture An advanced Treatise.* Academic Press, New York, San Francisco, London, 1971.